Seasonal and diurnal variations in Martian surface ultraviolet irradiation: biological and chemical implications for the Martian regolith

International Journal of Astrobiology 2 (1): 21–34 (2003) Printed in the United Kingdom
DOI: 10.1017/S1473550402001180

Seasonal and diurnal variations in Martian surface ultraviolet irradiation: biological and chemical implications for the Martian regolith

M.R. Patel[1]*, A. Bérces[2], C. Kolb[3], H. Lammer[3], P. Rettberg[4], J.C. Zarnecki[1] and F. Selsis[5]

[1]*Planetary and Space Sciences Research Institute, The Open University, Walton Hall, Milton Keynes MK7 6AA, UK*
e-mail: m.r.patel@open.ac.uk
[2]*MTA-SE Research Group for Biophysics, Semmelweis Med. University, VIII Puskin u.9, H-1444 Budapest, Hungary*
[3]*Space Research Institute, Department for Extraterrestrial Physics, Austrian Academy of Sciences, Schmiedlstr. 6, A-8042, Graz, Austria*
[4]*German Aerospace Centre (DLR), Institute of Aerospace Medicine, 51170 Cologne, Germany*
[5]*Centro de Astrobiologia (CSIC/INTA), Carretera Ajalvier, km 4, Torrejón de Ardoz, Madrid, Spain*

Abstract: The issue of the variation of the surface ultraviolet (UV) environment on Mars was investigated with particular emphasis being placed on the interpretation of data in a biological context. A UV model has been developed to yield the surface UV irradiance at any time and place over the Martian year. Seasonal and diurnal variations were calculated and dose rates evaluated. Biological interpretation of UV doses is performed through the calculation of DNA damage effects upon phage T7 and Uracil, used as examples for biological dosimeters. A solar UV 'hotspot' was revealed towards perihelion in the southern hemisphere, with a significant damaging effect upon these species. Diurnal profiles of UV irradiance are also seen to vary markedly between aphelion and perihelion. The effect of UV dose is also discussed in terms of the chemical environment of the Martian regolith, since UV irradiance can reach high enough levels so as to have a significant effect upon the soil chemistry. We show, by assuming that H_2O is the main source of hydrogen in the Martian atmosphere, that the stoichiometrically desirable ratio of 2:1 for atmospheric H and O loss rates to space are not maintained and at present the ratio is about 20:1. A large planetary oxygen surface sink is therefore necessary, in contrast with escape to space. This surface oxygen sink has important implications for the oxidation potential and the toxicology of the Martian soil. UV-induced adsorption of O_2^- super-radicals plays an important role in the oxidative environment of the Martian surface, and the biologically damaging areas found in this study are also shown to be regions of high subsurface oxidation. Furthermore, we briefly cover the astrobiological implications for landing sites that are planned for future Mars missions.

Received 4 April 2002, accepted 11 November 2002

Key words: biologically effective dose, DNA damage, landing sites, Mars, radiation climate, radiative transfer, regolith, toxicology, UV.

Introduction

The ultraviolet (UV) radiation climate at the surface of Mars is of significant importance in any astrobiological investigation. Radiation at these wavelengths (in the case of Mars 200–400 nm) is capable of interacting directly with biological structures and causing severe damage. Ultraviolet radiation also plays an important role in the photochemistry of atmospheres, and would be an important factor in the creation and persistence of highly oxidizing surface environments such as those found on Mars. High-intensity UV environments, especially in combination with oxidizing surface environments, can place restrictions on the survivability of biological organisms, strongly influencing evolution and effectively defining limiting lifetimes for species. Indeed, if the UV intensity in specific wavelength regions is high enough, the persistence of life can be made impossible for most forms of known biological organisms. During the early evolution of life on Earth, the UV radiation climate was different from that of present-day Earth. It can be assumed that during the Archaean era, during which the diversification of early anaerobes took place and the first anaerobic photosynthetic bacteria appeared (about 3.5 Gyr ago), the amount of free oxygen in the atmosphere was significantly lower than today. There was very little or no absorption of solar UV radiation by ozone. The strong influence of UV radiation on biological evolution is

* Corresponding author.

reflected by the appearance of different protection mechanisms in all terrestrial organisms such as enzymatic DNA repair, spore formation, UV-absorbing pigments, behavioural adaptation of motile organisms, and trapping and binding of sediments to form mats, etc.

In biological systems UV radiation causes temporary or permanent alterations that result from photochemical reactions of UV with different biological target molecules, the so-called chromophores (Rettberg & Rothschild 2001). The most important UV target in cells is DNA because of its unique role as genetic material and its high UV sensitivity. The absorbing parts of DNA are the bases, the purine derivatives adenine and guanine, and the pyrimidine derivatives thymine and cytosine. Although the base composition of DNA is different in different genes and organisms, there are common features of an absorption maximum in the 260 nm region and a rapid decline towards longer wavelengths. Absorption by proteins between 240 and 300 nm is much lower than that of nucleic acids of equal concentration. Most proteins are present in cells in higher numbers of identical copies. Therefore, photochemical alterations in only a fraction of them do not disturb their biological function significantly. The same is true for biological molecules such as unsaturated fatty acids, flavins, steroids, chinones, porphyrins or carotenoids, which serve as components of the cell membrane, coenzymes, hormones or electron donor transport molecules.

Leading DNA lesions particularly induced by short-wavelength UV components (UV-B, UV-C) of the solar spectrum are cyclobutane dimers, formed by two adjacent pyrimidine bases (Fisher & Johns 1976). Nucleic acids can be protected from UV radiation by various factors, which are able either to attenuate the radiation or restore the photoproducts. Attenuating factors can be proteins, H_2O or minerals, while restoration of the photoproducts can be performed by specific metabolic processes such as DNA repair or by the UV photons themselves in direct photoreversion.

Because of the importance of this relatively small region of the solar spectrum, it is useful when addressing such issues in astrobiology to place this UV environment in a biological context. The response of different biological structures to UV exposure are distinctly unique, and as such species-specific biological functions are required to correctly weight the irradiance spectrum in terms of biological damage. Since the effects of UV at different wavelengths vary so much from negligible to complete inactivation, the effect at all wavelengths must be weighted according to the damage it causes (Rettberg & Horneck 1999). This defines a biological weighting spectrum specific to the biological structure in question, which can then be applied to the UV spectrum proposed. By analysing the convolution of these two spectra, information on the effects of UV upon the organism under study can be estimated (Fig. 1).

The Martian UV environment has previously been investigated (Kuhn & Atreya 1979; Cockell *et al.* 2000; Lammer *et al.* 2001; Molina-Cuberos *et al.* 2001; Muller & Moreau 1991; Patel *et al.* 2002; Rontó *et al.* 2002), revealing a surface environment exposed to UV-C as low as 200 nm. This is in

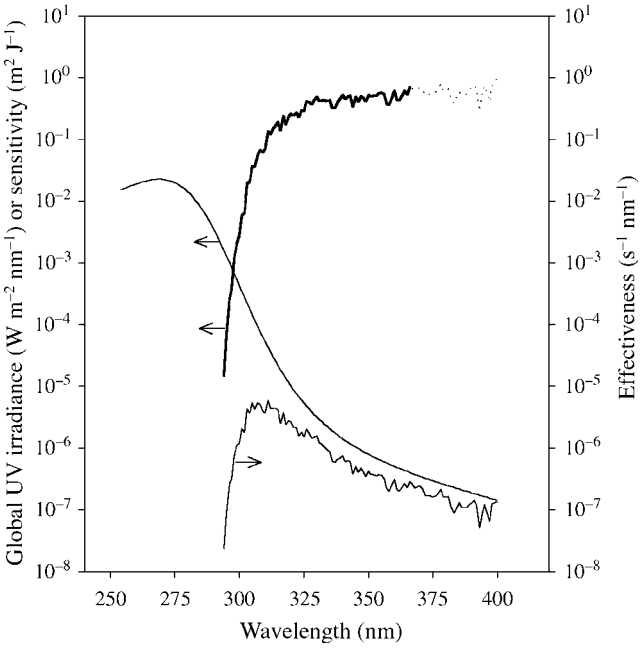

Fig. 1. Biological weighting of UV radiation: solar spectral irradiance at the Earth's surface, a biological weighting function (the absolute DLR-biofilm action spectrum, left axis) and the resulting solar effectiveness spectrum (right axis) (taken from Rettberg & Rothschild 2001).

stark contrast to the terrestrial case, where the ozone layer effectively screens all radiation <290 nm. Thus the biological response of organisms in the full 200–400 nm region needs to be known to accurately gauge the true biological effect of the UV environment. Presented here is an analysis of seasonal and diurnal variations of UV flux on the Martian surface, with associated biologically effective doses (BED) for two exemplary biological UV dosimeters. Bacteriophage T7 and polycrystalline Uracil thin layers are used on Earth for studies on DNA-based biological hazards and have proven useful for indicating the dependence of the biological end-effects on the radiation quality (Rontó *et al.* 1994; Fekete *et al.* 1998; Kerékgyarto *et al.* 1999; Rontó *et al.* 2000). The preparation and exposure of both biological dosimeters are described by Rontó *et al.* (1992) and Kerékgyártó *et al.* (1999).

T7 is a small double-stranded DNA molecule consisting of 39 937 base pairs, a protein core and a protein envelope (Rontó *et al.* 1983). Polycrystalline Uracil is considered as a model substance for studying UV-induced DNA damage by having Uracil bases, a natural component of RNA bases, in specifically suitable conformation for dimerization (Gróf *et al.* 1996) induced by solar UV radiation. A radiative transfer UV model has thus been developed covering a wide variety of Martian situations and environments, to which a range of biological responses can be applied to quantify these end effects.

The biological experiments on the Viking landers failed to detect any organic matter in the Martian soil, either at the surface or from samples collected a few centimetres below the surface (e.g. Klein *et al.* 1976). This result leads to the conclusion that strong oxidation processes are possibly at work

near the surface. Therefore, we also discuss the interaction between the Martian atmosphere and the chemical environment of the Martian regolith in relation to the modelled UV flux, where highly oxidizing regions can be created. The biological effects of these proposed oxidizing areas expected on the Martian surface through its orbital period are also discussed.

Mars UV model

Model structure

The method used here to model the Martian UV environment is based on that of Patel *et al.* (2002) (from here on referred to as Paper 1). For this study the radiative transfer model was significantly improved in a number of areas, allowing for a better representation of the actual Martian environment.

The Martian atmosphere was taken as 10 separate homogenous layers, consisting of a mixture of gas and aerosol particles distributed appropriately with altitude. All major atmospheric gas species are accounted for (CO_2, N_2, Ar, O_2, O_3, CO) in terms of scattering and absorption, though it should be noted that CO_2, O_2 and O_3 are the only significant absorbers in the wavelength region considered here. Absorption cross-sections for the above were taken as in Paper 1. Atmospheric gas was distributed between 0 and 200 km, with layer interfaces at 1, 5, 10, 15, 20, 21, 35, 50, 51 and 200 km. The column density of each atmospheric gas for each layer was easily determined through knowledge of partial pressure at the layer interface and the mean molecular mass (an assumption here is that the mean molecular mass is invariant with altitude). The column abundance of each individual species was then calculated from the total layer column abundance and mixing ratio of each species. Pressure as a function of altitude, used to determine each layer column abundance, was taken from Pathfinder entry data (Magalhaes *et al.* 1999). For the purposes of this study, the aerosols were assumed to consist solely of dust particles (ice aerosols are not considered here) and were confined to the lower 20 km of the atmosphere with a scale height equal to that of the atmospheric gas.

The Delta-Eddington approximation for radiative transfer (Joseph *et al.* 1976) was employed to determine the diffuse flux at the surface created by aerosol and molecular scattering. Composite scattering parameters (single-scattering albedo, asymmetry factor and extinction efficiency) were explicitly defined for each layer and the surface diffuse flux was calculated through simultaneous calculation of each layer's transmission equation.

Direct solar flux was determined via Beer's law exponential attenuation, again taking into account scattering and absorption from each species in each atmospheric layer. The direct flux was then added to the diffuse component to yield a total surface irradiance.

This process was performed at 1 nm intervals between 180 and 400 nm. The large abundance of CO_2 ($\sim$95%) coupled with its increasing absorption cross-section towards shorter wavelengths creates a distinct cut-off point in all Martian spectra, and thus no features below 200 nm are observed at the Martian surface. Sensitivity spectra for T7 and Uracil were then applied to each (λ dependent) UV flux value, yielding a Biologically Effective Dose (BED, addressed later).

Martian dust

The ubiquitous haze present in the Martian atmosphere is formed primarily of dust particles. High wind speeds, dust devils and local/global storms raise particulate matter from the surface of Mars, injecting it into the atmosphere. The dust remains present in the atmosphere for long periods of time, and plays a major role in global circulation and atmospheric dynamics. One resultant effect is the creation of a more isothermal troposphere through direct absorption of solar radiation into the atmosphere, altering temperature and pressure profiles significantly (Barth *et al.* 1992), consequently affecting the UV irradiance encountered at the surface. The amount of dust in the atmosphere thus has a non-trivial effect on the surface UV spectrum, and must be properly accounted for. The creation of a significant diffuse irradiance also must be considered whenever situations such as, for example, the possible survival of micro-organisms in permanently shadowed regions are investigated. The optical properties of the suspended dust need to be accurately known to quantify the nature and degree of interaction with solar radiation. The data of Ockert-Bell *et al.* (1997) were used, though as discussed previously in Paper 1 the issue of accurately defining the UV properties of Martian dust does remain an unresolved issue. At this time, however, these data remain the most complete dataset available for use.

The spatial and temporal variation of dust in the Martian atmosphere also needed to be defined, if annual variations were to be investigated. The distribution and amount of atmospheric dust is highly asymmetric when considered over the entire Martian orbit. This correlates well to the relatively high eccentricity of the Martian orbit, causing a corresponding change in (top of atmosphere) input solar irradiance from 717 to 493 W m^{-2} from perihelion to aphelion, respectively. This large difference in input solar energy to the Martian atmosphere is thought to be responsible for the variation in dust activity through the year (Kahn *et al.* 1992).

Dust activity is generally low towards aphelion when solar input is at its lowest at $L_s = 70^\circ$ (where L_s is the areocentric solar longitude, a measure of orbital position). Activity is seen to increase and peak at perihelion ($L_s = 250^\circ$), which is the expected time of year for possible large-scale dust events such as global dust storms (Pollack *et al.* 1979). Higher dust loadings are also experienced in the southern hemisphere at this time, when the local summer occurs.

Three annual dust variations were employed here, representing various degrees of UV attenuation. The dust scenarios utilized here are taken from the Mars Climate Database (MCD) by Lewis *et al.* (1999) and are available online at http://huchard.lmd.jussieu.fr/live_access/doc_htmls/data_set/node3.html. These consist of the following scenarios.

(1) Low dust scenario τ_{low}, where the dust optical depth (and thus dust loading) is spatially constant over latitude (lat) and temporally constant over L_s, and taken as $\tau = 0.1$.

(2) High dust scenario τ_{high}, where the optical depth is spatially constant over latitude but temporally dependent upon L_s, and is given as

$$\tau_{high} = 0.7 + 0.3\cos(L_s + 80^\circ). \quad (1)$$

This variation is a fit to the peak-removed variations as observed during the Viking years.

(3) Nominal dust scenario $\tau_{nominal}$, where τ is spatially dependent upon latitude and temporally dependent upon L_s. This scenario is taken from recent Mars Global Surveyor results, and is the best representation of the current nominal Mars dust environment. It is given as

$$\tau_{nominal} = \tau_N + (\tau_{eq} - \tau_N) \times 0.5 \times \{1 + \tanh[(45^\circ - \text{lat})/10]\} \quad \text{for lat} > 0 \quad (2)$$

$$\tau_{nominal} = \tau_S + (\tau_{eq} - \tau_S) \times 0.5 \times \{1 + \tanh[(45^\circ + \text{lat})/10]\} \quad \text{for lat} < 0 \quad (3)$$

where

$$\tau_{eq} = 0.2 + (0.5 - 0.2)\{\cos[(L_s - 250^\circ)/2]\}^{14} \quad (4)$$

$$\tau_S = 0.1 + (0.5 - 0.1)\{\cos[(L_s - 250^\circ)/2]\}^{14} \quad (5)$$

$$\tau_N = 0.1. \quad (6)$$

All three scenarios were run for each investigation, with scenarios 1, 2 and 3 each representing years of high, low and nominal UV exposures respectively.

Sensitivity spectra for BED

For quantification of the biological effects of UV radiation at the Earth's surface, simple organisms/micro-organisms (Tyrrell 1978; Munakata 1989; Quintern *et al.* 1992; Rettberg *et al.* 1998; Rettberg & Horneck 2000), bacterial viruses (Furusawa *et al.* 1990; Rontó *et al.* 1992), isolated nucleic acids (Regan *et al.* 1992) and nucleic acid bases (Gróf *et al.* 1996) have been used as biological UV dosimeters. Most of these techniques are based on the measurement and detection of DNA damage or its consequences. Bacteriophage T7 and Uracil thin-layer dosimeters were developed and improved for assessment of the DNA-based biological hazard on Earth (Rontó *et al.* 1994; Fekete *et al.* 1998). These dosimeters also proved to be suitable for indicating the dependence of the biological end effects on the type of UV radiation (Rontó *et al.* 2000), and were thus used in the present BED study for Mars.

The BED is determined as the weighted spectrum integrated over wavelength and time to give a weighted total UV dose as shown in equation (7):

$$\text{BED} = t \sum_{\lambda} F(\lambda) S(\lambda) \Delta\lambda, \quad (7)$$

where t is the duration of exposure in seconds, F is the flux at wavelength λ and S is the sensitivity weighting factor at wavelength λ for the biological effect under consideration.

$S(\lambda)$ was constructed for both species from Modos *et al.* (1999), and is given as

$$S(\lambda) = a \exp[-b_1(\lambda - \lambda_0)] \quad \text{if } \lambda < \lambda_0 \quad (8)$$

and

$$S(\lambda) = a \exp[-b_2(\lambda - \lambda_0)] \quad \text{if } \lambda > \lambda_0, \quad (9)$$

where a, b_1, b_2 and λ_0 are constants taken from Table 1 of Modos *et al.* (1999). Unfortunately, the direct experimental data of Modos *et al.* (1999) exist only down to 250 nm. Since the Martian UV range extends down to 200 nm, a polynomial fit of $S(\lambda)$ to DNA damage from the experimentally determined data of Hieda (1994) between 250 and 200 nm was used. Once $S(\lambda)$ was defined for the full wavelength region, the BED rate could be calculated for any modelled UV situation. Biologically effective dose data are calculated for 1 s, i.e. both diurnal and annual variations are expressed in dose rates and can be compared with the terrestrial values.

Results

Diurnal variations

Shown here are diurnal variations of the instantaneous BED for T7 and Uracil. Two extreme cases are investigated; Fig. 2 shows high BED at perihelion (southern summer) and Fig. 3 shows low BED at aphelion (southern winter). As well as total BED, the separate contributions of direct and diffuse BED irradiance are also shown. The diffuse dose experienced by organisms in possible shadowed regions can now also be evaluated. Diffuse levels are fairly substantial, making protection via shadowing a more complicated issue. The general shape of the diurnal profiles between perihelion and aphelion are similar, but dose values vary markedly. Also, the increased daytime period is evident towards perihelion, escalating further the total daily dose.

Annual variations

The surface UV exposure for each annual dust scenario was modelled and the BED for both T7 and Uracil was calculated. The annual plots for the nominal and high dust cases are shown in Figs 4 and 5, where the flux along a pole-to-pole latitude strip at 7.5 mbar and local noon was calculated at each L_s throughout the Martian year, and thus shows the dose near midday from north to south pole along a line of constant pressure, geographically representative only of latitude.

The distinct asymmetry in the plot is a result of two combined effects, namely the relatively high eccentricity of the Martian orbit and the obliquity of Mars' planetary axis. Eccentricity creates an asymmetry in L_s, where perihelion forms a concentrated dose region (hotspot), and obliquity creates the asymmetry in latitude, shifting the hotspot into the southern hemisphere. Also evident are the negligible dose regions at high latitudes, where the polar night effect is experienced in both hemispheres.

The differences caused by the dust scenarios are subtle, but worth commenting upon. The plots for low and nominal dust

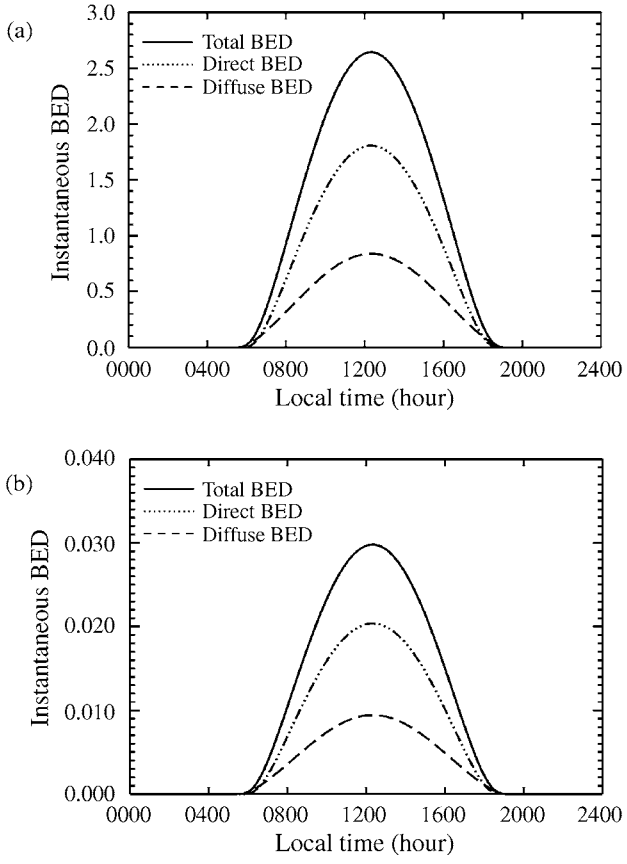

Fig. 2. Total, direct and diffuse BED diurnal variations at perihelion for $L_s = 250°$, latitude = 20° S at a pressure of 7.5 mbar: (a) shows the profile for T7 and (b) shows the Uracil profile.

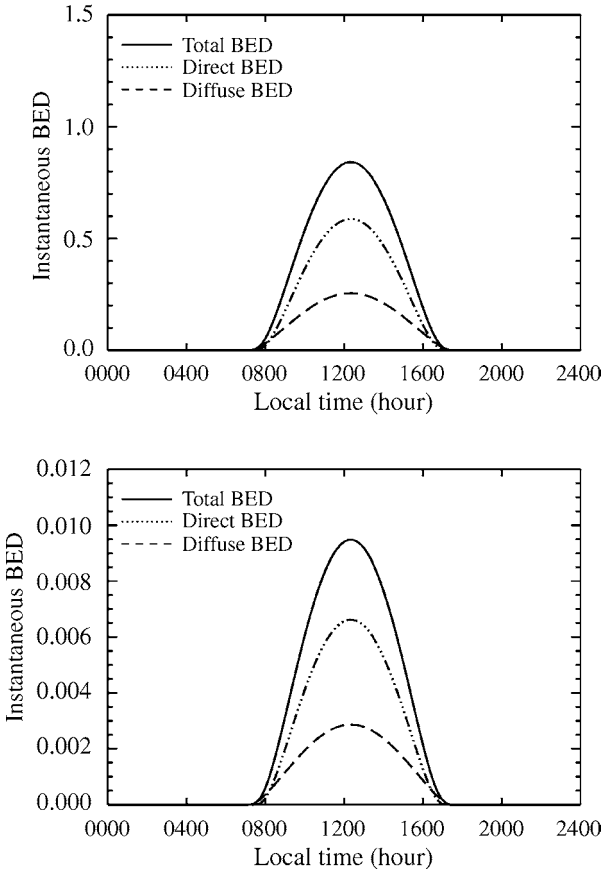

Fig. 3. Total, direct and diffuse diurnal BED variations at aphelion for $L_s = 70°$, latitude = 30° S at a pressure of 7.5 mbar: (a) shows the profile for T7 and (b) shows the Uracil profile.

levels are spatially and temporally the same, except for the difference in absolute dose amounts (thus the low dust plot is omitted). The low dust scenario, as expected, creates the highest dose levels (~15% higher than nominal in terms of surface flux) as less dust in the atmosphere allows for greater penetration of UV to the surface. A different annual variation is observed in the high dust scenario (Fig. 5), with the hotspot spread out in the equatorial region throughout most of the Martian year.

In the two other scenarios, the hotspot is more defined, occurring at perihelion in the southern hemisphere, indicating that the presence of larger amounts of suspended dust in the atmosphere throughout the year spreads this effect both spatially and temporally. Periods of maximum exposure thus occur at a different point in the orbit. In the low and nominal cases maximum exposure occurs in the southern hemisphere at perihelion, intuitively consistent with a relatively optically thin atmosphere. In the high dust case however, maximum atmospheric dust loading occurs at perihelion counteracting the increased solar flux, and as a result the maximum exposure occurs instead just prior to perihelion around $L_s = 200°$. The effect of dust in the atmosphere in this case upon the radiative transfer of UV radiation is thus shown here to dominate over solar input variation throughout the Martian orbit.

Biological interpretation

In order to determine how harmful the solar UV radiation at the Martian surface for biological organisms could be, we compared the BED diurnal variations at perihelion and aphelion of Figs 2 and 3 with two extreme cases on Earth, namely Antarctica and at the equator (Fig. 6). Fig. 2 shows the total, direct and diffuse BED diurnal variations at Martian perihelion for $L_s = 250°$ and latitude of 20° S at a pressure of 7.5 mbar. Curve A shows the profile for the biological sensor T7, and curve B for Uracil. Fig. 3 shows the same scenario at aphelion for $L_s = 70°$ and latitude = 30° S. Fig. 6 shows a diurnal case during the spring equinox (March 21st) at the terrestrial equator, with an ozone concentration of 220 Dobson units (DU). The terrestrial UV fluxes and BED rates were determined using the radiative transfer model of Green *et al.* (1974) for typical atmospheric aerosol conditions. The latitude-dependent terrestrial ozone values were taken from NASA's Total Ozone Mapping Spectrophotometer (TOMS) website (http://jwocky.gsfc.nasa.gov/TOMSmain.html).

It is interesting to note that the maximum instantaneous total diurnal BED values in both Martian cases (Figs 2 and 3) are higher than terrestrial values at the equator. The Martian perihelion diurnal BED value for T7 is about 900 times greater than the value at Earth's equator, and about 300 times greater

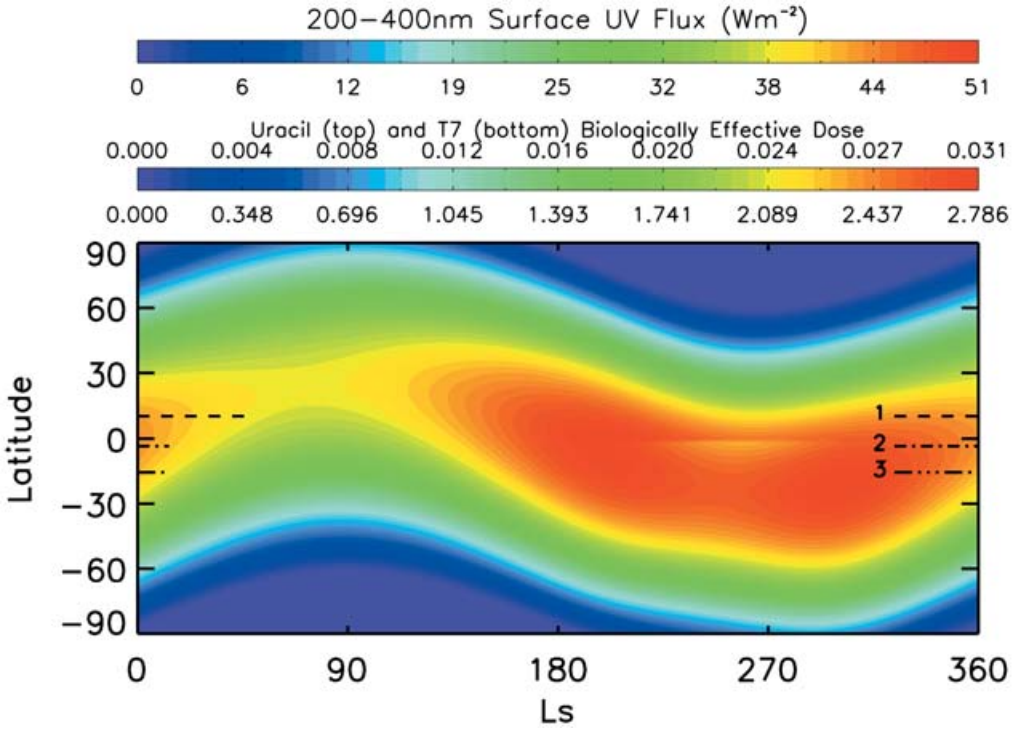

Fig. 4. Annual variations of UV for the nominal dust scenario. The surface flux, T7 BED and Uracil BED are all shown. Also shown are the locations of two expected Martian landers: (1) shows the Beagle 2 landing site, operating at 10.6° N from $L_s = 322°$ to 053°; (2) shows a possible Mars Exploration Rover (MER) landing site in Terra Meridiani at 2° S, $L_s = 325°$ to 012°; (3) shows a second possible MER site in Gusev Crater, for similar L_s at 14.8° S.

at aphelion (shown in Fig. 3). For Uracil we obtain total BED values at Martian perihelion that are about 3000 times greater than at the Earth's equator, and for Martian aphelion the values are about 900 times greater. The instantaneous BED rates for Antarctica, latitude = 90° S, with a very low ozone concentration of 80 DU (http://jwocky.gsfc.nasa.gov/TOMSmain.html) are 3.6×10^{-4} for T7 and 1.2×10^{-6} for Uracil. These values are about 10 times larger than the instantaneous BED rates for those at the Earth's equator. However, the spectral irradiances involved in the Martian and terrestrial cases are very different. As shown by Rontó *et al.* (1997) the ratio between BED^{T7}/BED^{U} of the integrated BED rates for T7 and Uracil over the whole day depends on the spectral distribution of the radiation source. The reason for this dependence is the higher sensitivity of Uracil in the UV-B and UV-C short-wavelength regions compared with T7. Since the short-wavelength radiation is absorbed on Earth by the global ozone layer but can penetrate the thin Martian atmosphere, one obtains much lower BED^{T7}/BED^{U} ratio values on Mars compared with Earth.

Measured terrestrial BED^{T7}/BED^{U} ratios in Budapest, Hungary (latitude = 47.5° N, longitude = 19° E) with an ozone concentration of 322 DU are about 430 during June (summer solstice) and about 780 in December (winter solstice). The values for BED^{T7}/BED^{U} ratios for both terrestrial extreme cases described above are about 300. The solar UV irradiance is much larger at the equator than at Antarctica, but low ozone concentrations in Antarctica imply greater UV-B penetration. The similarity between the terrestrial ratios at the equator and the Antarctic area occur because the radiation must penetrate through a larger atmospheric mass in Antarctic regions than at the equator. The longer path of the light rays through the atmosphere diffuses the UV radiation, resulting in a lower net surface irradiation. For both Martian cases we obtain very low BED^{T7}/BED^{U} ratios of about 100. The much lower value is caused mainly by the biologically hostile solar UV-C flux and implies high DNA damage rates on the present Martian surface. One can see from Figs 4 and 5 that the surface UV irradiation and the BED rates are much lower during the Martian year at latitudes higher than 45° N and 60° S, as a result of lower UV exposure of the Martian surface at these latitudes. Since UV-C radiation also penetrates to the surface at high latitudes, the values for the BED^{T7}/BED^{U} ratios are comparable to lower latitudes, also resulting in a biologically hostile surface environment. From Figs 4 and 5 one can also see that the polar caps are the areas with the lowest UV irradiation levels and thus lowest BED rate environmental conditions on Mars. Although ice is less effective at providing protection from UV radiation than dust or rock, at sufficient depths the penetrating solar UV radiation will be attenuated. Studies in Antarctica using a 254 nm source for measuring the penetration of UV-C radiation into ice showed that at a depth of 1 cm of ice, the biologically hostile UV-C radiation is reduced by 40% and at a depth of 5 cm about 90% of the UV-C radiation is attenuated (Nienow *et al.* 1988; Cockell 2001). The study of Nienow *et al.* (1988) indicates that the

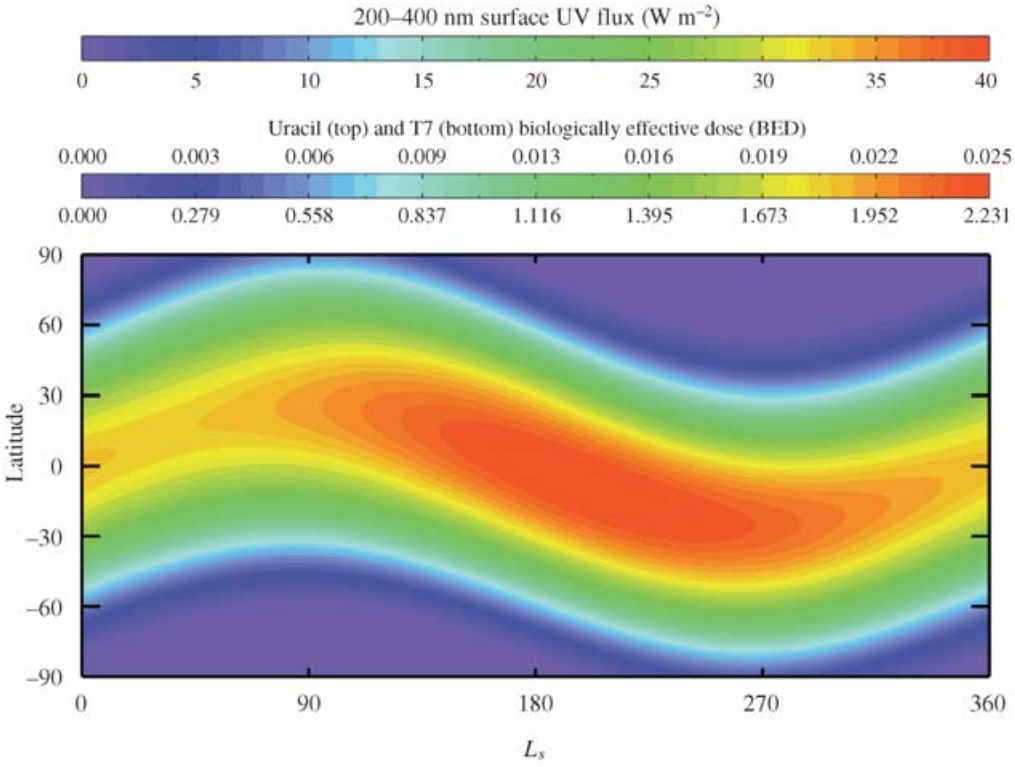

Fig. 5. Annual variations of UV for the high dust scenario. The surface flux, T7 BED and Uracil BED are all shown. The difference in annual distribution of the UV flux compared with the nominal case is readily apparent.

majority of the dangerous UV-C radiation should be absorbed within the first few centimetres under the surface at the Martian north pole.

Since photosynthetic microbes survived at the surface on early Earth before the atmosphere developed a protective ozone layer, they would have required tolerance to UV-C, UV-B and UV-A radiation (e.g. Wynn-Williams & Edwards 2001). Recent studies showed that the survival of UV stress by certain micro-organisms (i.e. Notoc, Gloeocapsa and other cyanobacterial species that are common in UV-exposed Antarctic habitats) might be due partly to their carotenoid content. It is likely that UV radiation influences carotenoid synthesis by lichens, which are symbioses of fungi and either cyanobacteria or algae. Carotenoids that were isolated from Antarctic lichens showed considerable variation in content throughout the whole season, requiring care to standardize conditions for inter-site comparisons (Wynn-Williams & Edwards 2001). For example, β-carotene is one of several pigments that can absorb hostile UV-C radiation. Generally, such attributes are no longer required in the present terrestrial atmosphere, and these capabilities of certain micro-organisms may be a relic property from their early evolution before the terrestrial surface was protected by ozone, i.e. from conditions similar to how Mars is now. Dust storms reduce the intensity of the incoming solar UV irradiation on the surface locally or globally, but do not fully protect the surface enough from the DNA-damaging UV-C wavelengths. Biological matter that gets under or into rocks should be well protected if the soil or rocks contain no chemical radicals that may destroy organic molecules. Therefore, in the next section we study the oxidation process of the Martian surface caused by the atmosphere–surface interaction.

Oxidation/chemical environment of regolith

The discovery of organic molecules in Martian soil or rocks by future Mars landers would be of great importance for the search of life on Mars. Unfortunately NASA's Viking landers were unable to detect evidence of life on Mars, but found a chemically reactive soil capable of decomposing organic molecules (e.g. Klein *et al.* 1976; Yen *et al.* 2000b). This reactivity was attributed to the presence of inorganic superoxides or peroxides in the upper Martian soil. Recent laboratory experiments by Yen *et al.* (2000a) indicate that superoxide radical ions such as O_2^- form directly on Mars-analogue mineral surfaces when exposed to UV radiation under simulated Martian atmospheric conditions. These oxygen radicals can explain the reactive environment of the Martian soil and the absence of organic material in the upper surface layers. There is much evidence from atmospheric evolution studies that atmospheric oxygen interacts with the Martian surface environment (Lammer *et al.* 1996, 2002). The escape of hydrogen and oxygen from the Martian atmosphere has important implications for the chemistry of the atmosphere. We assume that the main source of escaping hydrogen is Martian H_2O from exchangeable subsurface ice reservoirs:

$$2H_2O \rightarrow 2H_2 + O_2 \qquad (10)$$

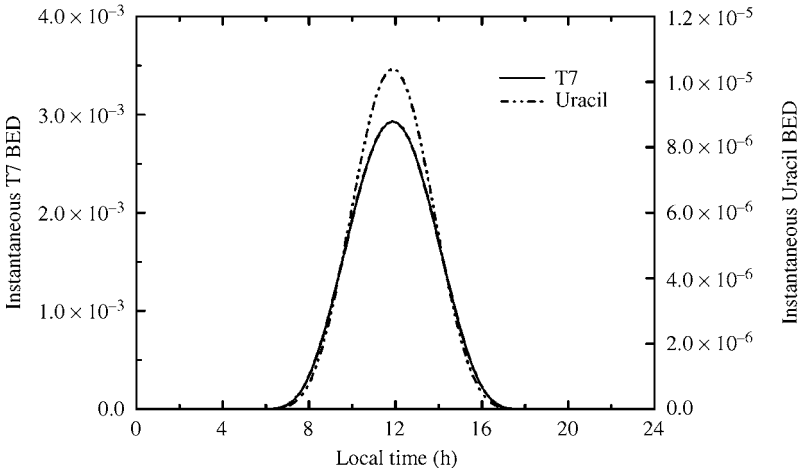

Fig. 6. Terrestrial total diurnal BED variations for T7 and Uracil at the equator, latitude = 0° at spring equinox, for an ozone concentration of 220 DU.

Each loss of two H_2 molecules leaves behind one O_2 molecule. If there were no permanent sinks for oxygen, the oxygen concentration in the Martian atmosphere would continue to build up. If the Martian atmosphere has reached a steady state for its state of oxidation, there must be a sink for oxygen comparable in magnitude to the escape flux of hydrogen, i.e.

$$\Phi_H = 2\Phi_O, \tag{11}$$

where Φ_H is the escape flux of hydrogen and Φ_O is the escape flux of oxygen in any form from the Martian atmosphere. Mariner 6 and 7 UV spectrometers observed the Lyman-α emission of atomic hydrogen in an altitude range between 200 and 24 000 km (Anderson & Hord 1971). They obtained thermal escape rates for atomic hydrogen of about $1.5 \times 10^{26}\ s^{-1}$. Recent observations with the Far Ultraviolet Spectroscopic Explorer (FUSE) satellite of molecular hydrogen in the Martian atmosphere yielded molecular hydrogen escape rates of about $1.7 \times 10^{24}\ s^{-1}$ (Krasnopolsky & Feldman 2001). Lichtenegger & Dubinin (1998) and Lammer *et al.* (2002) estimated the non-thermal loss rates of H^+ and H_2^+ ions using a test particle model, which involves the motion in the interplanetary electric and magnetic field. They found total hydrogen ion escape rates for moderate solar wind conditions of the order of about $7.5 \times 10^{25}\ s^{-1}$, which agrees well with observed Phobos 2 results (Lundin *et al.* 1990a, b). Using the current observed and modelled thermal and non-thermal hydrogen escape rates one arrives at a total average loss of hydrogen atoms from present-day Mars of about $2.3 \times 10^{26}\ s^{-1}$. If the stoichiometrically desirable ratio of 2:1 of H and O loss rates to space are obtained one would require a total O loss rate to space of about $1.15 \times 10^{26}\ s^{-1}$. If this ratio is not maintained an additional permanent oxygen sink for establishing the 2:1 ratio is required, which is most likely UV-driven chemical reactions with the Martian soil.

Unfortunately, oxygen is too heavy to escape thermally from Mars via the Jeans escape process. However, there are several non-thermal atmospheric loss processes that can yield the escape of oxygen from the Martian exosphere. Since Mars does not have an appreciable intrinsic magnetic field at present, the atmosphere can be eroded by particle sputtering and solar wind pick-up processes. Dissociative recombination of molecular oxygen ions is also known to lead to loss of atomic constituents where the gravitational potential on Mars is easily overcome by the energy imparted in the production of hot atoms (Fox & Dalgarno 1983; Lammer & Bauer 1991; Fox 1993; Lammer *et al.* 1996, 2000, 2002; Fox & Bakalian 2001). Estimated values for the current oxygen escape flux owing to dissociative recombination, sputtering and pick-up processes cover a very wide range of 3.0×10^6 to $1.2 \times 10^8\ cm^{-2}\ s^{-1}$ between low and high solar wind conditions (e.g. Lammer & Bauer 1991; Fox 1993; Zhang *et al.* 1993; Luhmann 1997; Kass & Yung 1995, 1996, 1999; Johnson & Liu 1996; Lammer *et al.* 1996, 2000, 2002; Johnson *et al.* 2000; Fox & Bakalian 2001; Leblanc & Johnson 2001). Fox (1997) estimated the theoretical upper limit to the outflow of all oxygen ions if all ions produced above the photochemical equilibrium region could be lost, and derived an escape flux of $1.2 \times 10^8\ cm^{-2}\ s^{-1}$. It is important to also note that this flux value is too low for establishing the present Martian stoichiometrically desirable ratio of 2:1 of H and O loss rates to space. On the other hand, it is unlikely that the present Martian atmosphere has an average atmospheric oxygen escape flux of the order of $10^8\ cm^{-2}\ s^{-1}$, since such a high value could only be reached theoretically in the past when solar activity was much higher. Using realistic model values for average non-thermal oxygen escape rates results in dissociative recombination oxygen loss rates of about $2.3–5 \times 10^{24}\ s^{-1}$ (Lammer & Bauer 1991; Fox 1993), for atmospheric sputtering of oxygen atoms about $6.5 \times 10^{23}\ s^{-1}$ (Leblanc & Johnson 2001), for CO_2 molecules about $3.0 \times 10^{23}\ s^{-1}$ and for pick-up processes about $9.5 \times 10^{24}\ s^{-1}$ (Lammer & Bauer 1991; Lichtenegger & Dubinin 1998; Lammer *et al.* 2002).

One can see from the average total oxygen loss rate of about $1.0 \times 10^{25}\ s^{-1}$ that the stoichiometrically desirable ratio of 2:1 of H and O escape to space is not maintained, and at

present the ratio is about 20:1. Lammer *et al.* (1996) estimated a ratio of about 12:1, corresponding to the higher oxygen and CO_2 sputtering loss rates based on one-dimensional (1D) sputtering models. Leblanc & Johnson (2001) developed a modified three-dimensional (3D) test particle model that describes the sputtered particle population and the escaping particles inside the hot oxygen corona. Furthermore, the heating effect due to the incident particle flux is described in their simulations by using a two-dimensional (2D) direct simulation Monte Carlo model. Their results show that the standard 1D models used by earlier estimations overestimate the sputtering yields by about 15–25 % when they are corrected for coronal ejections. This result implies that oxygen loss to space cannot be the dominant oxygen removal mechanism on Mars. According to the present escape rate of hydrogen, photolysis of H_2O will produce the observed oxygen concentration in the Martian atmosphere in just 10^5 yr, making a large planetary oxygen sink necessary. Accordingly, it appears that the missing oxygen needed for validating the total 2:1 ratio between H and O as described in equation (11), which is not lost to space, is incorporated into the surface by chemical weathering processes that oxidize the Martian soil.

For estimating the oxygen potential in the Martian regolith one must know how long the 2:1 ratio between H and O to space was not maintained. Lammer *et al.* (1996, 2002) studied the evolution of hydrogen and oxygen loss rates throughout Martian history. One can see from their results that the oxygen in the Martian atmosphere has been interacting with the surface for at least approximately 1 Gyr. Fig. 6 shows the evolution of hydrogen and oxygen loss rates during the past 3.5 Gyr. The loss rates are based on model results of Fox (1993), Johnson & Luhman (1998), Leblanc & Johnson (2001) and Lammer *et al.* (2002). One can see that the total oxygen loss rate to space is lower compared with the total hydrogen loss rate expressed in H_2 since at least 1 Gyr ago. Previously, more oxygen was lost from the Martian atmosphere than hydrogen since the solar wind was denser and atmospheric erosion processes were more active in the past. In such a case, self-regulation between H and O loss as proposed by McElroy & Donahue (1972) and Liu & Donahue (1975) may enhance the loss of hydrogen. In this case the oxygen concentration of the atmosphere will decrease owing to its higher loss rate. This causes an increase in the production of H_2 in the atmospheric HO_x chemistry, resulting in a greater escape rate for hydrogen, so that a new steady state would be reached which would satisfy equation (11).

There are several studies that investigated the decomposition of organic materials due to O_2^- adsorption (Lunsford 1984; Gasymov *et al.* 1984; Llewellyn Jones *et al.* 1978; Alvarez 1996; Yen *et al.* 2000b). Organic molecules are not only destroyed directly by solar UV radiation but also by its derivatives, such as superoxide ions. Even during night or at greater soil depths where water adsorption dominates the chemical environment, perhydroxyl and hydroxyl radicals liberated by the reaction given above are capable of oxidizing putative organic materials. An important parameter for the evaluation of the oxidation of organics is the oxidant extinction depth, at which the concentration of the oxidizing agents reaches zero owing to its chemical interaction with the subsurface environment (Zent 1998). If any putative organism vulnerable to enlarged oxygen fugacity is present within the Martian soil, then this is the minimum depth to which sampling must occur to have a good chance of detecting possible extant organic material. As mentioned before, the Viking results showed that 10 cm beneath the Martian surface the soil was devoid of organic material. At this depth the oxidant should have reached roughly 75 % of its primary concentration if one assumes an oxidant extinction depth of about 2.5 m (75 % is related to the assumption of 2.5 m). The lack of organic material at these depths tends to indicate that fossilized organics also decompose in the subsurface environment. The probability of finding fossilized remains also depends on the effect of meteoritic gardening. Zent (1998) investigated this effect on the basis of hydrogen peroxide diffusion. We use the results of the oxygen surface sink as shown in Fig. 7 in combination with data from the model given in Zent (1998) for the estimation of the Martian regolith depth in comparison with estimated values from the Mars Orbital Camera (MOC) on-board the Mars Global Surveyor (MGS) spacecraft (Gilmore 1999). The oxidant that is responsible for the oxidation of organic materials on Mars is thought to also be a key reactant for the soil oxidation process itself. To estimate the effect on the evolution of the Martian regolith, a phenomenological study – disregarding the oxidation process itself – was performed, taking several assumptions into account. The overall, irreversible oxygen surface sink based on atmospheric evidence (Lammer *et al.* 1996, 2002) as discussed before, results in approximately 2×10^{42} O particles being incorporated into the Martian surface over the past 1 Gyr.

From multispectral data of the Mars Pathfinder Imager it is known that the proportion of ferric iron at the landing site is up to 95 % (Morris *et al.* 2000). Martian magmatic precursing rocks (basalts, andesites) exhibit a certain amount of initial ferric iron due to the oxygen fugacity in the differentiated magma. The values for Martian meteorites and lunar mare basalts are obtained by the investigation of magmatic feldspar (Dyar *et al.* 2001):

$$\frac{n_{Fe^{3+}}}{n_{Fe,\,tot}} = X_{Fe^{3+},\,i} = \begin{matrix} 0.00 \text{ SNC QUE } 94201 \\ 0.23 \text{ Lunar mare basalt } 15555 \\ 0.53 \text{ SNC Zagami.} \end{matrix} \qquad (12)$$

Iron is a common trace element in feldspar, and because of its small amount the influence of the crystallographic site on the ferrous/ferric distribution is thought to be negligible. Martian meteorites undergo two impact processes, so it cannot be ruled out that the ferric/ferrous ratio has been shifted since the formation of these rocks. Only two values for Martian basaltic meteorites are available, and the range is very large. Moreover, because the oxygen fugacity in the rocks on the Moon is unaffected by any atmospheric process, lunar values should represent reasonable values – even for Mars.

Almost all iron in the Martian soil is in state III – this could only be generated by oxidation of ferrous iron in addition to

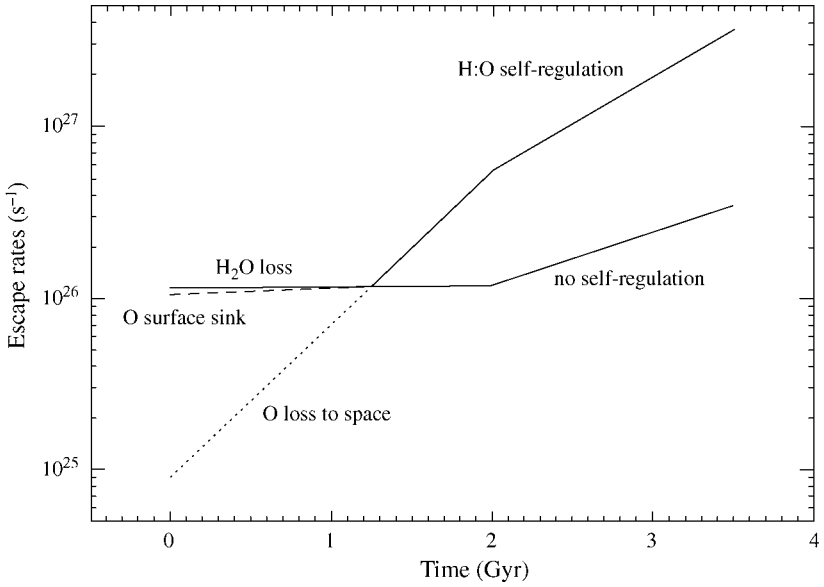

Fig. 7. Atmospheric loss rates of hydrogen and oxygen during the past 3.5 Gyr. One can see that the total oxygen loss rate to space is lower compared to the total hydrogen loss rate (in H_2) since at least 1 Gyr. For maintaining the total 2:1 ratio between H and O, atmospheric oxygen that is not lost to space is incorporated into the surface by chemical weathering processes and is responsible for oxidizing the Martian regolith.

metallic and sulphidic meteoritic iron. The net reaction to satisfy the facts given above is thus:

$$\underset{\text{ferrous phases}}{2FeO} + 0.5O_2 \xrightarrow{h\nu} \underset{\text{ferric phases.}}{Fe_2O_3} \tag{13}$$

An even more important effect for an irreversible oxygen surface sink is the formation of sulphates. A moderate approach is the formation of kieserite ($MgSO_4 \cdot H_2O$) through reaction with sulphitic volcanic gases:

$$Mg(OH)_2 + SO_2 + 0.5O_2 \rightarrow MgSO_4 \cdot H_2O. \tag{14}$$

Another model reaction is the generation of sulphates from the oxidation of meteoritic sulphides (mainly pyrrhotite, FeS):

$$2FeS + 4.5O_2 + 7H_2O \rightarrow Fe[SO_4/OH] \cdot 3H_2O. \tag{15}$$

We calculated an iron content of the Martian soil of about 13 wt% and a sulphur content of about 2 wt% from Rieder *et al.* (1997). The density of the soil was set to a value of 1.5 g cm^{-3}.

An important boundary condition to evaluate the oxygen surface sink is the effect of meteoritic gardening. Fresh material will be brought up to the surface and oxidized matter will be buried during this process (Zent 1998). The meteoritic size–frequency distribution functions given in Neukum & Ivanov (1994) and in Carr (1981) are assumed to represent meteoritic production functions in the time period of our interest. The period of about 1 Gyr since the onset of oxidation up to now is not compatible with Noachian distribution functions (dominated by deep impacts; Carr 1981) and Chryse distribution functions (dominated by shallow impacts; Dial 1978).

A further parameter within the models is the expected oxidant extinction depth. 2 m and an extrapolated value of 5 m were used for this value in this context. Meteoritic ejecta are assumed to become oxidized during thermal activity within the Martian atmosphere. We used Figs 6 and 7 published in Zent (1998), and confined in our model 10 vol% of the regolith as Martian rocks. Fig. 8 shows our results in terms of the Martian regolith depth versus the final ferric/ferrous oxidation state. The estimation of the regolith depth based on impact geometry by means of MOC data on-board the MGS amounts to a range of between 20 and 113 m (Gilmore 1999). Neukum production functions linked with a 2 m oxidant extinction depth resulted (even with sulphatic production from sulphides) in several hundred metres of regolith. Using the same parameters but with an extinction depth of 5 m, more reasonable values for the regolith depth are yielded. Using the Carr production function and 2 m extinction depth gives a regolith depth of several metres. Since new models of meteoritic size–frequency distribution functions (Head *et al.* 2001) indicate populations within the Carr and Neukum range, our calculation shows that an oxidant extinction depth of about 2 m may represent a minimum value. Depending on the assumptions, we propose a range of between 2 and 4 m for the oxidation depth.

More detailed studies are planned in the future where we incorporate experimental studies into a comprehensive model for the soil formation process on Mars. The following parameters can thus lead to a decrease of the regolith depth:

(1) domination of deep impacts;
(2) higher oxidant extinction depth (several kinds of strong oxidants, aeolian gardening);
(3) formation of sulphates entirely from meteoritic sulphidic matter;
(4) meteoritic ejecta becoming oxidized during impacts.

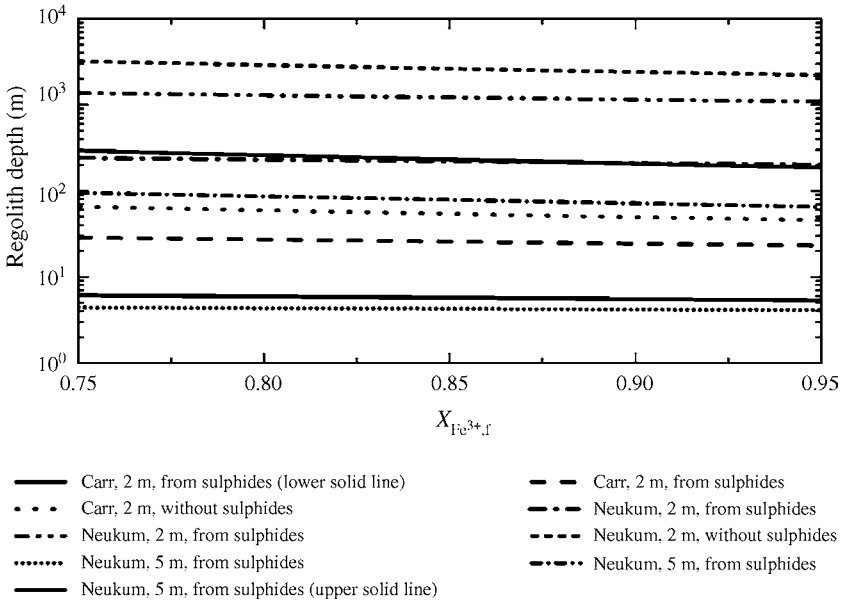

Fig. 8. Martian regolith depth versus the final ferric/ferrous oxidation state with different meteoritic production functions.

To decide whether or not a fully inorganic process driven by photochemical processes is sufficient to explain the global oxygen surface sink, experimental studies are required. However, solar-UV induced oxidation of metallic iron under Martian conditions seems to be an active process (Yen 1999). The red areas relating to the surface irradiation of solar UV flux on the contour plots in Figs 4 and 5 show areas where the induced surface oxidation processes should act with their greatest efficiency. However, Martian dust storms can distribute surface dust over the entire planet, so that oxidized constituents can also reach areas at higher latitudes including the polar caps. Areas related to high production rates of adsorbed superoxides may also be areas where adsorbed superoxide ions may diffuse into the subsurface. Therefore, higher latitudes may be covered with oxidized dust, but diffusion of superoxides into the subsurface should not be as effective as at the main production areas.

Adsorbed superoxide ions, such as O_2^- are thought to be responsible for the chemical reactivity of the Martian soil. It was shown by means of experimental studies under Martian conditions that UV irradiation, atmospheric oxygen, very low water concentrations and mineral grain surfaces are the main elements in the formation process of this adsorbate (Yen *et al.* 2000a). Solar UV radiation excites the mineral substrate material liberating electrons to the grain surfaces. These electrons are incorporated in free oxygen, which forms O_2^- adsorbates (Ito *et al.* 1985). Because these ions are formed progressively under intense UV irradiation one can assume that solar UV photons are not a limiting factor in this oxidant production process – as is the case for H_2O_2. Hunten (1979) has proposed H_2O_2 as a possible 'standard' Martian oxidant owing to its formation in the atmosphere and soil (Huguenin 1982). Arguments against H_2O_2 as the major soil oxidant are: first, the short lifetime against UV destruction on the Martian surface and, secondly, that H_2O_2 alone cannot explain the thermally stable gas exchange experimental results of the Viking biological experiments (Bullock et al. 1994). It seems that the concentration of superoxide oxygen radicals is governed mainly by the amount of adsorbed water (Cotton *et al.* 1995):

$$2O_2^- + H_2O \downarrow \rightarrow O_2 \uparrow + HO_2^- + OH^-. \quad (16)$$

This reaction is held at a certain equilibrium of adsorbed radicals and free adsorbed water and oxygen in the near-surface atmosphere. Superoxide radicals should also be able to diffuse into deeper parts of the Martian regolith and may be responsible for the reactivity of the Viking soil samples from depths of around 10 cm. Two-dimensional diffusion of superoxide radicals was observed on material surfaces (Clarkson & Kooser 1978; Yen *et al.* 2000a). Since the radicals are strongly adsorbed owing to their charging, they are able to remain adsorbed on particles during transport. Aeolian and meteoritic gardening is therefore an important process in enhancing the capability of reaching greater depths.

Space exposure experiments related to toxicology and UV protection

In order to test the potential toxicity and protection against solar UV radiation of Martian soil analogues, highly resistant terrestrial organisms were used: spores of the soil bacterium *Bacillus subtilis*. In the dormant stage, spores undergo no detectable metabolism and exhibit a high degree of resistance to inactivation by various different physical stresses, such as cycles of extreme heat and cold, extreme desiccation including vacuum, UV and ionizing radiation, as well as oxidizing agents or corrosive chemicals (reviewed by Nicholson *et al.* 2000). In the presence of appropriate nutrients, spores respond rapidly by germination and outgrowth, resuming vegetative growth. Hence, spore formation represents a strategy by which

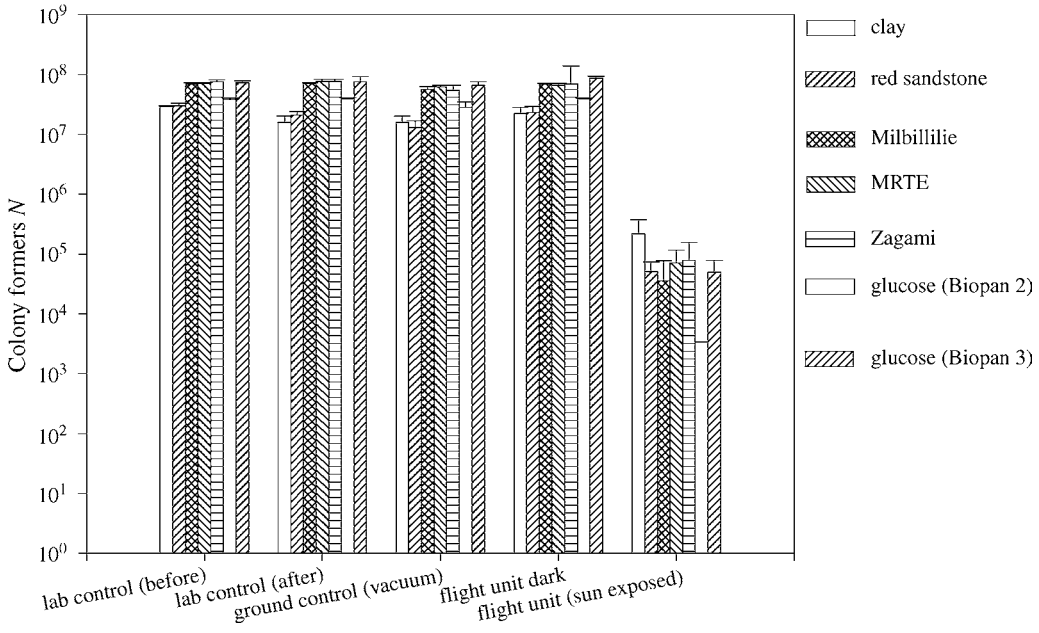

Fig. 9. Survival of *B. subtilis* spores (strain HA101) exposed to vacuum and solar UV radiation in space in the presence of protective material: clay, sandstone, glucose, Martian soil analogue (MRTE) and samples of two meteorites, Zagami from Mars and Milbillilie, probably from Vesta.

a bacterium escapes temporally and/or spatially from unfavourable conditions. Among the bacterial spores, the endospores of the genus *Bacillus* are the best investigated. Their response to the conditions of space has been studied in several space experiments (reviewed by Horneck 1993) as well as in studies using space simulation facilities (Horneck 1999). In a series of three space experiments in the ESA facility BIOPAN on a Russian satellite the protective and/or toxic effect of minerals, e.g. Martian soil analogues and samples of real Martian meteorites, under the influence of solar UV radiation were investigated (Horneck *et al.* 2001). In Fig. 9, results with bacterial spores dried and mixed with different compounds and exposed to space vacuum and solar UV radiation are shown in comparison with samples exposed to space vacuum only, as well as compared with ground control experiments. Here the effects of added clay, sandstone, glucose, Martian soil analogue (MRTE) and samples of two real meteorites (Zagami from Mars and Milbillilie, probably from Vesta) on the survival of the spores were studied. From the results of these BIOPAN experiments in space, it can be concluded that the tested compounds do not show toxic effects, either in ambient air or in vacuum. If bacterial spores are exposed to solar UV radiation, a reduction of survival by about six orders could be measured under these conditions due to the lethal effects of UV radiation (data not shown, Horneck *et al.* 2001). However, in the presence of protective compounds survival is reduced only by three orders of magnitude. Concerning the surface of Mars, results indicate that even thin layers of Martian dust may be able to protect organisms against the deleterious effects of UV radiation including the short-wavelength ranges of UV-C and UV-B (>200 nm) which do not occur on Earth today.

Proposed sites for future Mars landing sites

The effects of UV on the oxidation state of the surface and on eventual complex organics or biological molecules have strong implications on the strategy for Mars exploration. The landing sites of future Martian missions are chosen to compromise engineering constraints and scientific objectives. Two of the strongest constraints are the availability of solar power and the avoidance of extremely low temperatures. These two parameters define the latitude boundaries that allow correct operation of the scientific and communication instruments. In the case of the 2003 Mars Exploration Rovers (MER) the landing sites have to be located within 15° S–5° N (MER-A) and 10° S–10° N (MER-B, which will land 52 sols after MER-A). The two final sites for these rovers will be chosen between Hematite in Terra Meridiani (2.07° S) and Melas Chasma in Valles Marineris (8.88° S). Gusev crater (14.8° S), Isidis Planitia (4.31° N), Thabasca Vallis (8.92° N) and Eos Chasma (13.34° S) are also possible back-up sites. The MERs will land towards the beginning of 2004; they will carry geological sensors and collect data that will be used as ground truth for the remote sensing observations from orbiters (MGS, Mars Odyssey and future missions). At the same time, the Beagle 2 lander will land in the Isidis region, at 10.6° N, carrying an array of astrobiological equipment designed to search for signs of life, and will offer a third ground reference point for orbiting spacecraft. As discussed earlier, there should be a strong link between the oxidation state of surface material and the UV flux. However, for obtaining detailed information concerning the UV effects upon oxidation levels, the variation and efficiency of adsorbates as well as a qualitative estimation of the relationship between surface UV levels, temperature, pressure and oxidation levels must be achieved. Detailed laboratory

experiments on Martian soil analogues under simulated Martian atmospheric conditions will be performed in the near future at the Space Research Institute of the Austrian Academy of Sciences.

Moreover, any ground mission with astrobiological objectives such as searching for biological surface activity or its remnants will face the same problem: on one hand, the need for solar radiation as an energy source for instrumentation and, on the other hand, the need for low solar exposure because of the biological effect of UV radiation and the indirect oxidation it induces. Therefore, landing at extreme latitudes is required to provide a complete geological ground truth and to perform astrobiological *in situ* studies at the Martian surface. Such landing sites (such as previously planned for the Mars Polar Lander) would of course face technical challenges, such as working and communicating with a low power supply and low temperatures. Hence, our present work and forthcoming studies will help to select future landing sites and also to determine to what extent the data collected *in situ* can be considered as a reference for interpreting remote observations.

Conclusions

Continued development of a radiative transfer code to model ultraviolet transmission through the Martian atmosphere has resulted in the possibility of investigating seasonal and diurnal variations in Martian surface UV flux and its associated consequences. From the orbital geometry, a UV 'hotspot' is seen to form at mid-southern latitudes towards perihelion, altering in position and season depending upon the annual dust scenario under investigation. Suspended dust is shown to have a significant effect on the surface UV flux, and thus must be properly accounted for in any astrobiological situation. The BED experienced on Mars is shown to be biologically harmful; absolute levels are far higher in the Martian case when compared with Earth, and the ratio of the T7 and Uracil BED values highlights the damaging effect of the short-wavelength UV-C penetrating through to the Martian surface. The effect of UV creating an oxidative environment is also shown as an important factor for astrobiological investigations. The O_2 sink presented creates a harsh oxidizing environment in the Martian regolith through UV interactions, and its depth determines the extent to which investigation must occur in order to find traces of life. Possible biological protection has been shown to be provided via potential Martian dust layers that can partially reduce the incoming solar UV flux in the biologically relevant UV-B and UV-C regions. Possible future landing site strategies for Mars landers have also been discussed, highlighting the need for high-latitude missions away from high levels of biologically damaging UV and subsurface oxidation activity.

Acknowledgements

M.R.P. acknowledges funding from PPARC (UK) for this work as part of a PhD project, and would like to thank Greg Bodeker for his valuable advice on radiative transfer. The authors thank Gy. Rontó for discussions regarding BED rates. H.L., C.K. and A.B. thank the Österreichischer Akademischer Austauschdienst (ÖAD) for supporting this work, which is part of the Austrian-Hungarian ÖAD-project A-20/2000: Effect of Extraterrestrial Radiation on Molecules Essential for Life.

References

Alvarez, B. (1996). *Chem. Res. Toxicol.* **9**, 390–396.
Anderson, D.E. & Hord, C.W. (1971). *J. Geophys. Res.* **76**, 6666–6673.
Barth, C.A., Stewart, I.F., Bougher, S.W., Hunten, D.W., Bauer, S.J. & Nagy, A.F. (1992). *Mars*, ed. Kieffer, H.H., Jakosky, B.M., Snyder, C.W., Matthews, M.S., pp. 1054–1089. University of Arizona Press, Tuscon, AZ.
Bullock, M.A., Stoker, C.R., McKay, C.P. & Zent, A.P. (1994). *Icarus* **107**, 142–154.
Carr, M.H. (1981). *The Surface of Mars*, p. 232. Yale University Press, New Haven, CT.
Clarkson, R.B. & Kooser, R.G. (1978). *Surf. Sci.* **74**, 325–332.
Cotton, F.A., Wilkinson, G. & Gaus, P.L. (1995). *Basic Inorganic Chemistry*, pp. 435–443. Wiley, New York.
Cockell, C.S. (2001). *Astrobiology*, ed. Horneck, G. & Baumstark-Khan, C., pp. 219–230. Springer-Verlag, Berlin.
Cockell, C.S., Catling, D.C., Davis, W.L., Snook, K., Kepner, R.L., Lee, P. & McKay, C.P. (2000). *Icarus* **146**, 343–359.
Dial, A.L. (1978). *NASA Tech. Memo.*, 79729, pp. 179–189.
Dyar, M.D., Delaney, J.S. & Tegner, C. (2001). *32nd Annual Lunar and Planetary Science Conf. Houston, TX*, abstract no. 1065.
Fekete, A., Vink, A.A., Gáspár, S., Bérces, A., Módos, K., Rontó, Gy. & Roza, L. (1998). *Photochem. Photobiol.* **68**, 527–531.
Fisher, G.J. & Johns, H.E. (1976). *Photochemistry and Photobiology of Nucleic Acids*, ed. Wang, S.Y., pp. 226–294. Academic Press, New York.
Furusawa, Y., Suzuki, K. & Sasaki, M. (1990). *J. Radiation. Res.* **31**, 189–206.
Fox, J. & Dalgarno, T.M. (1983). *J. Geophys. Res.* **88**, 9027–9032.
Fox, J. (1993). *Geophys. Res. Lett.* **20**, 1847–1850.
Fox, J. (1997). *Geophys. Res. Lett.* **24**, 2901.
Fox, J. & Bakalian, F.M. (2001). *J. Geophys. Res.* **106**, 28 785–28 795.
Gasymov, A.M., Przhevalskaya, L.K., Shvets, V.A. & Kazanskii, V.B. (1984). *Kinetics Catalysis* **25**, 293–297.
Gilmore, M.S. (1999). *5th Int. Conf. on Mars, Pasadena, CA*, abstract no. 6228.
Green, A.E.S., Sawada, T. & Shettle, E.P. (1974). *Photobiol.* **19**, 251–259.
Gróf, P., Gáspár, S. & Rontó, Gy. (1996). *Photochem. Photobiol.* **64**, 800–806.
Head, J.W., Greeley, R., Golombek, M.P., Hartmann, W.K., Hauber, E., Jaumann, R., Masson, P., Neukum, G., Nyquist, L.E. & Carr, H. (2001). *Space Sci. Rev.* **96**, 263–292.
Hieda, K. (1994). *Int. J. Radiat. Biol.* **66**, 561–567.
Horneck, G. (1993). *Orig. Life Evol. Biosphere* **23**, 37–52.
Horneck, G. (1999). *Laboratory Astrophysics and Space Research*, ed. Ehrenfreund, P., Krafft, C., Kochan, H. & Pirronello, V., pp. 667–685. Kluwer, Dordrecht.
Horneck, G., Rettberg, P., Reitz, G., Wehner, J., Eschweiler, U., Strauch, K., Panitz, C., Starke, V. & Baumstark-Khan, C. (2001). *Orig. Life Evol. Biosphere* **31**, 527–547.
Huguenin, R.L. (1982). *J. Geophys. Res.* **87**, 10 069–10 082.
Hunten, D. (1979). *J. Mol. Evol.* **14**, 57–64.
Ito, T., Kato, M., Toi, K., Shirakawa, T., Ikemoto, I. & Tokuda, T. (1985). *J. Chem. Soc., Faraday Trans.* **81**, 2835–2844.
Johnson, R.E. & Liu, M. (1996). *Science* **274**, 1932.
Johnson, R.E. & Luhmann, J.G. (1998). *J. Geophys. Res.* **103**, 3649–3653.
Johnson, R.E., Schnellenberger, D. & Wong, M.C. (2000). *J. Geophys. Res.* **105**, 1659–1670.

Joseph, J.H., Wiscombe, W.J. & Weinman, J.A. (1976). *J. Atmos. Sci.* **33**, 2452–2459.
Kahn, R.A., Martin, T.Z., Zurek, R.W. & Lee, S.W. (1992). *Mars*, ed. Kieffer, H.H., Jakosky, B.M., Snyder, C.W. & Matthews, M.S., pp. 1017–1053. University of Arizona Press, Tuscon, AZ.
Kass, D.M. & Yung, Y.L. (1995). *Science* **268**, 697–699.
Kass, D.M. & Yung, Y.L. (1996). *Science* **274**, 1932–1933.
Kass, D.M. & Yung, Y.L. (1999). *Geophys. Res. Lett.* **26**, 3653–3656.
Kerékgyártó, T., Gróf, P. & Rontó, Gy. (1999). *J. Photochem. Photobiol.* B **53**, 27–35.
Klein, H.P. *et al.* (1976). *Science* **194**, 99–105.
Krasnopolsky, V.A. & Feldman, P.D. (2001). *Science* **294**, 1914–1917.
Kuhn, W.R. & Atreya, S.K. (1979). *J. Mol. Evol.* **14**, 57–64.
Lammer, H. & Bauer, S.J. (1991). *J. Geophys. Res.* **96**, 1819–1825.
Lammer, H., Stumptner, W. & Bauer, S.J. (1996). *Geophys. Res. Lett.* **23**, 3353–3356.
Lammer, H., Stumptner, W. & Bauer, S.J. (2000). *Planet. Space Sci.* **48**, 1473–1478.
Lammer, H., Molina-Cuberos, G.J., Stumpner, W., Kargl, G., Selsis, F., Kerékgyártó, T. & Berces, A. (2001). *ESA-SP* **496**, 363–366.
Lammer, H., Lichtenegger, H., Kolb, C., Ribas, I. & Bauer, S.J. (2002). *J. Geophys. Res.* submitted.
Leblanc, F. & Johnson, R.E. (2001). *Planet. Space Sci.* **49**, 645–656.
Lewis, S.R., Collins, M., Read, P.L., Forget, F., Hourdin, F., Fournier, R., Hourdin, C., Talagrand, O. & Huot, J.P. (1999). *J. Geophys. Res.* **104**, 24 177–24 194.
Lichtenegger, H. & Dubinin, E. (1998). *Earth Planets Space* **50**, 445 – 452.
Liu, S.C. & Donahue, T.M., *Icarus* **28**, 231–246.
Llewellyn Jones, D.T., Knight, R.J. & Gebbie, H.A. (1978). *Nature* **274**, 875–878.
Luhmann, J.G. (1997). *J. Geophys. Res.* **102**, 1637–1638.
Lundin, R., Zakhrov, A., Pellinen, R., Barabash, S.W., Borg, H., Dubinin, E.M., Hulquist, B., Koskinen, H., Liede, I. & Pissarenko, N. (1990a). *Geophys. Res. Lett.* **17**, 873–876.
Lundin, R., Zakharov, A., Pellinen, R., Borg, H., Hultquist, B., Pissarenko, N., Dubinin, E.M., Barabash, S.W., Liede, I. & Koskinen, H. (1990b). *Geophys. Res. Lett.* **17**, 877–880.
Lunsford, J.H. (1984). *Am. Chem. Soc. Sympos. Ser.* Vol. 248, pp. 127–142.
Magalhaes, J.A., Schofield, J.T. & Seiff, A. (1999). *J. Geophys. Res.* **104**, 8943–8955.
McElroy, M.B. & Donahue, T.M. (1972). *Science* **177**, 986–988.
Modos, K., Gaspar, S., Kirsch, P., Gay, M. & Ronto, Gy. (1999). *J. Photochem. Photobiol.* B **49**, 171–176.
Molina-Cuberos, G.J., Stumptner, W., Lammer, H., Kömle, N.I. & O'Brien, K. (2001). *Icarus* **154**, 216–222.
Morris, R.V. *et al.* (2000). *J. Geophys. Res.* **105**, 1757–1817.
Muller, C. & Moreau, D. (2001). *ESA-SP* **496**, 375–378.
Munakata, N. (1989). *J. Radiation Res.* **30**, 338–351.
Neukum, G. & Ivanov, B.A. (1994). *Hazards Due to Comets and Asteroids*, ed. Gehrels, T., pp. 359–416. University of Arizona Press, Tuscon, AZ.
Nicholson, W.L., Munakata, N., Horneck, G., Melosh, H.J. & Setlow, P. (2000). *Microbiol. Mol. Biol. Rev.* **64**, 548–572.
Nienow, J.A., McKay, C.P. & Friedmann, E.I. (1988). *Microbial Ecol.* **16**, 271–289.
Ockert-Bell, M.E., Bell, J.F., III, Pollack, J.B., McKay, C.P. & Forget, F. (1997). *J. Geophys. Res.* **102**, 9039–9050.
Patel, M.R., Zarnecki, J.C. & Catling, D.C. (2002). *Planet Space Sci.* **50**, 915–927.
Pollack, J.B., Colburn, D.S., Flaser, F.M., Kahn, R., Carlston, C.E. & Pidek, D. (1979). *J. Geophys. Res.* **84**, 2929–2945.
Quintern, L., Horneck, G., Eschweiler, U. & Bücker, H. (1992). *Photochem. Photobiol.* **55**, 389–395.
Regan, J.D., Carrier, W.L., Gucinski, H., Olla, B.L., Yoshida, H., Fujimura, R.K. & Wicklund, R.I., *Photochem. Photobiol.* **27**, 35–42.
Rettberg, P. & Horneck, G. (1999). *J. Epidemiol.* **9**, S-78–83.
Rettberg, P., Horneck, G., Strauch, W., Facius, R. & Seckmeyer, G. (1998). *Adv. Space Res.* **22**, 335–339.
Rettberg, P. & Horneck, G. (2000). *Adv. Space Res.* **26**, 2005–2014.
Rettberg, P. & Rothschild, L.J. (2001). *Astrobiology, the Quest for the Conditions of Life*, ed. Horneck, G., Baumstark-Khan, C., pp. 233–243. Springer-Verlag, Berlin.
Rieder, R., Economou, T., Wänke, H., Turkevich, A., Crisp, J., Brückner, J., Dreibus, G. & McSween, H.Y., Jr (1997). *Science* **278**, 1771–1774.
Rontó, Gy., Agmalyan, M.M., Drabkin, G.M., Feigin, L.A. & Lvov, Yu. M. (1983). *Biophys. J.* **43**, 309–314.
Rontó, Gy., Cáspár, S. & Bérces, A. (1992). *Photochem. Photobiol.* B **12**, 285–294.
Rontó, Gy., Gáspár, S., Gróf, P., Bérces, A. & Gugolya, Z. (1994). *J. Photochem. Photobiol.* **59**, 209–214.
Rontó, Gy., Bérces, A., Gáspár, S. & Gróf, P. (1997). *Eastern Europe and Global Change*, ed. Ghazi, A., Mathy, P. & Zerefos, C., pp. 99–110. EC, Brussels, Luxembourg.
Rontó, Gy., Bérces, A., Gróf, P., Fekete, A., Kerékgyarto, T., Gáspár, S. & Stick, C. (2000). *Adv. Space Res.* **26**, 2021–2028.
Rontó, Gy., Bérces, A., Lammer, H., Cockell, C.S., Molina-Cuberos, G.J., Patel, M.R. & Selsis, F. (2003). *Photochem. Photobiol.* **77**(1), 1–7.
Tyrrell, R.M. (1978). *Photochem. Photobiol.* **27**, 571–579.
Wynn-Williams, D.D. & Edwards, H.G.M. (2001). *Astrobiology*, ed. Horneck, G. & Baumstark-Khan, C., pp. 245–258. Springer-Verlag, Berlin.
Yen, A.S. (1999). *5th Int. Conf. on Mars, Pasadena, CA*, abstract no 6076.
Yen, A.S., Kim, S.S., Hecht, M.H., Frant, M.S. & Murray, B. (2000a). *Science* **289**, 1909–1913.
Yen, A.S., Kim, S.S., Freeman, B.A. & Hecht, M.H. (2000b). *LPSC XXXI*, abstract no. 1713.
Zent, A.P. (1998). *J. Geophys. Res.* **103**, 31 491–31 498.
Zhang, M.H.G., Luhmann, J.G., Nagy, A.F., Spreiter, J.R. & Stahara, S.S. (1993). *J. Geophys. Res.* **98**, 10 915–10 923.